

## Quantum paraelectricity versus ferroelectricity: Nonlinear polarizability model

A. Bussmann-Holder<sup>1</sup> and A. R. Bishop<sup>2</sup>

<sup>1</sup>Max-Planck-Institute Solid State Research, Heisenbergstr. 1, D-70569 Stuttgart, Germany

<sup>2</sup>Los Alamos National Laboratory, Theoretical Division, Los Alamos, New Mexico 87545, USA

(Received 22 January 2004; published 20 July 2004)

The suppression of ferroelectricity by quantum fluctuations is investigated within a nonlinear polarizability model. A mass dependence of the quantum fluctuation dominated state is discovered which can extend to rather high temperatures as compared to known quantum paraelectrics. In addition a crossover from order-disorder to displacive dynamics is observed when ferroelectricity is suppressed. A phase appears in a regime where deviations from the high-temperature behavior set in, where polar precursors coexist with paraelectric quantum fluctuations. Elastic stiffness is found to crucially contribute to mode-mode coupling and the stability of the system.

DOI: 10.1103/PhysRevB.70.024104

PACS number(s): 77.80.-e, 77.80.Bh, 63.70.+h, 63.20.Kr

Polar dielectrics have been a field of intense research for many decades because of their enormous potential for applications.<sup>1</sup> In this regard, mainly the huge static dielectric constants  $\epsilon_0$  are of interest, which are intimately related to the dynamical properties of the system. A limiting factor for applications is the strong temperature dependence of  $\epsilon_0$ . Recently enormous progress has been achieved here with the discovery of the perovskite-based system  $\text{CaCu}_3\text{Ti}_4\text{O}_{12}$ , which exhibits a nearly temperature-independent dielectric constant over a broad temperature regime and does not show any lattice instability.<sup>2</sup> A similar stabilization of the dielectric constant is known to take place in quantum paraelectrics, e.g.,  $\text{SrTiO}_3$  (Ref. 3) and  $\text{KTaO}_3$ ,<sup>4</sup> where complete mode softening is suppressed by quantum fluctuations. A stabilization of the soft mode at small frequencies and consequently large dielectric constants is observed over extended temperature regimes, since here the temperature is an ineffective parameter and the system reacts only upon changing direct or higher order interactions.<sup>4</sup> In this quantum limit the effective dimensionality is enhanced to  $D=4$ .<sup>5</sup> The unexpected finding of isotope-induced ferroelectricity in  $\text{SrTiO}_3$  (Ref. 6) has renewed the interest in the quantum fluctuation dominated regime, since conventional anharmonic lattice interaction models predict the absence of any isotope effect on  $T_c$ . Its origin is still debated, but a consistent explanation has been given in Ref. 7, where it has been shown that in the quantum regime, with the ineffectiveness of temperature, an anomalous mass dependence of the effective potential sets in, favoring a lattice instability.

Here we focus on this regime and investigate the *competition* between ferroelectricity and quantum paraelectricity in perovskite-type ferroelectrics. This regime has also previously been investigated theoretically, where a phenomenologically derived equation has been proposed in Ref. 8 to account for the deviations from the high-temperature regime. An approach based on an  $n$ -component vector model for structural phase transitions has been presented in Ref. 9, where specifically the critical exponents have been shown to change discontinuously in the limit  $n \rightarrow \infty$ . Here we use the nonlinear polarizability model in its simplest diatomic linear chain representation,<sup>10</sup> where the  $\text{BO}_3$  unit is represented by a polarizable cluster mass  $m_1$  while the  $A$  sublattice is given

by the rigid ion mass  $m_2$ . The model has various advantages as compared to *ab initio* approaches, e.g., first principles methods<sup>11</sup> or effective Hamiltonian approaches,<sup>12</sup> since it is parameter free, highly transparent, and, to a large extent, analytically tractable. It also reproduces, in quantitative agreement with experimental data, many temperature-dependent dynamical properties.<sup>13</sup> The success of the model is based on the fact that *electron-lattice* interactions are explicitly incorporated. Those have long been believed to be irrelevant to ferroelectric systems, since these are mostly insulators with a band gap of several eV. The importance of electron-phonon interactions in ferroelectrics, however, is based on the fact that small charge transfer between the oxygen ion  $p$  and transition metal  $d$  states triggers the soft mode dynamics and induce an anisotropic charge distribution favoring the polar state.<sup>14</sup> Phenomenologically this is incorporated in a shell model representation where a nonlinear core shell coupling at  $m_1$  is considered.<sup>15</sup> This coupling consists of an attractive harmonic term  $g_2$  and a fourth order repulsive term  $g_4$  which tend to compensate each other with decreasing temperature. Lattice stability is guaranteed by a second nearest-neighbor core-core coupling  $f'$  between the polarizable units, whereas the nearest-neighbor coupling  $f$  is through the shells only. Since the double well potential defined through  $g_2$  and  $g_4$  is in the relative core shell displacement coordinate at  $m_1$  and site  $n$ , i.e.,  $w_{1n}$ , which defines an integrated dipole moment, the exact solutions of the model differ considerably from conventional  $\Phi_4$ -type models. In the continuum limit kink, breather, and traveling pulse excitons exist<sup>16</sup> and in the lattice case nonlinear periodic wave solutions have been found<sup>17</sup> together with pseudoperiodic displacement patterns on new length scales accompanied by charge ordering.<sup>18</sup>

A very convenient way to study the quantum paraelectric and ferroelectric states is provided by using the self-consistent phonon approximation (SPA), which corresponds to a cumulant expansion of the third order term in  $w_{1n}$  in the equations of motion<sup>7,10</sup>

$$g_2 w_{1n} + g_4 w_{1n}^3 = w_{1n} (g_2 + 3g_4 \langle (w_{1n})^2 \rangle_T) = g_T w_{1n} \quad (1)$$

with

$$\langle (w_{1n})^2 \rangle_T = \sum_{q,j} \frac{\hbar}{2N\omega_{q,j}} w_1^2(q,j) \coth \left[ \frac{\hbar\omega_{q,j}}{2k_B T} \right], \quad (2)$$

where all dynamical information is provided through the SPA eigenvalues and corresponding eigenvectors  $\omega_{q,j}, w_1(q,j)$  for phonon branch  $j$  and all wave vectors  $q$ . The phase transition temperature is defined by the condition  $g_T = 0$ , i.e.,

$$\frac{|g_2|}{3g_4} = \sum_{q,j} \frac{\hbar}{2N\omega_{q,j}} w_1^2(q,j) \coth \left[ \frac{\hbar\omega_{q,j}}{2k_B T_c} \right]. \quad (3)$$

In this approximation the temperature dependent soft mode frequency is given by

$$\mu\omega_f^2(q=0) = \frac{2fg_T}{(2f + g_T)}, \quad (4)$$

where  $\mu$  is the unit cell reduced mass. While  $g_2$  and  $g_4$  have to be determined self-consistently,  $f$  and  $f'$  are obtained from the experimental optic and acoustic zone boundary frequencies which are explicitly given by

$$\begin{aligned} \omega_{\text{TO}}^2(q=2\pi/a) &= 2f/m_2, \omega_{\text{TA}}^2(q=2\pi/a) \\ &= 1/m_1[4f' + \mu\omega_f^2(q=0)]. \end{aligned}$$

In addition measurements of the elastic constants provide further information on  $f'$ . It is important to note here, that at high temperatures and in the limit  $m_1 \gg m_2$  the soft mode is localized with zero group velocity approaching the value  $\omega_f^2 = 2f/m_2$ . In this limit each atom is independent of its neighbors and feels only the surrounding electron gas. This corresponds to a large value of  $g_T$  and a large amount of screening. With decreasing temperature the ions begin to interact with each other and transfer energy to their neighbours to finally become acoustic phonons with frequency  $\omega_f^2 = 4f/m_2 \sin^2(qa)$  when the limit  $g_T = 0$  is reached. Simultaneously the acoustic mode is strongly depressed when  $m_1 \gg m_2$  and  $T$  is large and starts interacting with the soft mode with decreasing temperature, which results in anomalies in the elastic properties of the system. In addition, for high  $T$  the shell is infinitely separated from its core and the ion fully ionized, while for decreasing temperature localization sets in and charge density wave formation becomes possible.

In the quantum regime the limit  $g_T = 0$  is never fulfilled since the lattice instability is suppressed by quantum fluctuations. Using Eqs. (4) and (2) this limit can be investigated as a function of the double-well potential barrier height, and typical results for the soft mode frequency as function of temperature are shown in Fig. 1. The barrier height is relevant to the transition mechanism, as deep wells correspond to the order-disorder limit while shallow wells are typical for the displacive limit. Thus  $g_2$  has been limited to small values to guarantee that the displacive limit is realized.

In all the cases we investigated the soft mode frequency saturates at low temperatures by quantum fluctuations and is nearly independent of temperature for a rather broad regime which increases with decreasing barrier height. Simultaneously, a nearly parallel shift in the soft mode frequency to higher values is observed. This is due to the fact that the

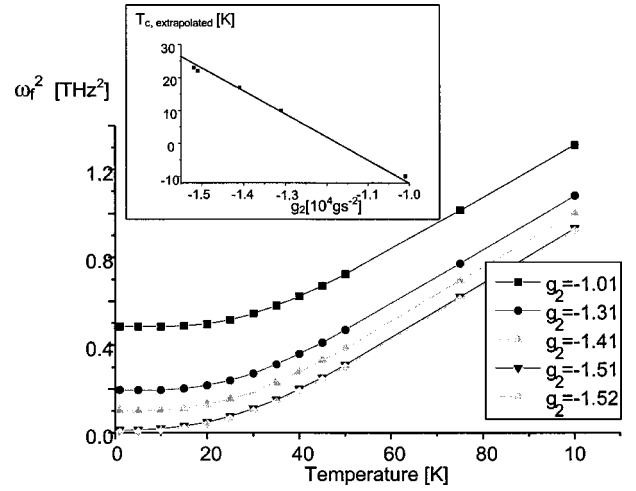


FIG. 1. Temperature dependence of the square of the soft mode frequency for varying potential barrier height. The inset shows the high temperature extrapolated  $T_{c,\text{extrapolated}}$  as function of  $g_2$ . Note that the observed seemingly trivial linear relation between  $T_{c,\text{extrapolated}}$  and  $g_2$  does not persist at very high temperatures where saturation of the soft mode frequency sets in (Ref. 10).

self-consistently derived value of  $g_T$  increases with decreasing barrier height. This increase is caused by the fact that the dipole moment defined by Eq. (2) decreases faster than  $g_T$  indicating increased electron localization. The parallel shifts of the soft mode frequency to higher values with decreasing potential barrier height demonstrate that the barrier height in the displacive limit does not affect the Curie constant. Extrapolating the linear in temperature regime of the soft mode frequency to zero yields the high-temperature extrapolated  $T_{c,\text{extrapolated}}$ , which is shown as a function of  $g_2$  in the inset of Fig. 1, and the expected linear relation between both is observed. From Fig. 1, it is obvious that a certain critical value of  $g_2$  exists at which the ferroelectric transition takes place. In the above example, transitions take place for all values of  $|g_2| > 1.52$ .

The mass dependence of the soft mode in the quantum regime is shown in Figs. 2 and 3. While in our previous calculations<sup>7</sup> on isotope induced ferroelectricity only the influence of the isotope substitution has been presented, we show here a systematic study of the variations of  $m_1$  in the quantum regime. We see that variations of the polarizable mass  $m_1$  have very different effects on the dynamics than those of the rigid ion mass  $m_2$ . Increasing  $m_1$ , the soft mode shifts to smaller frequencies and the system is closer to a lattice instability,<sup>9</sup> as observed in isotope-substituted  $\text{SrTiO}_3$ .<sup>6</sup> The soft mode shifts have a parallel behavior here, i.e., the Curie constant does not change with increasing mass, while the high-temperature extrapolated  $T_c$  is strongly mass dependent. Note that neither  $m_1\omega_f^2$  nor  $\mu\omega_f^2$  are constant at any temperature, as expected from harmonic theories, but a nonlinear variation with both is observed for small  $m_1$  which saturates at large masses only (see inset to Fig. 2). This observation is important to isotope effects on  $T_c$  which are unconventional in the small  $m_1$  limit. Varying the rigid ion sublattice mass  $m_2$  has different effects on the soft mode, since here the extrapolated  $T_c$  is nearly independent of  $m_2$

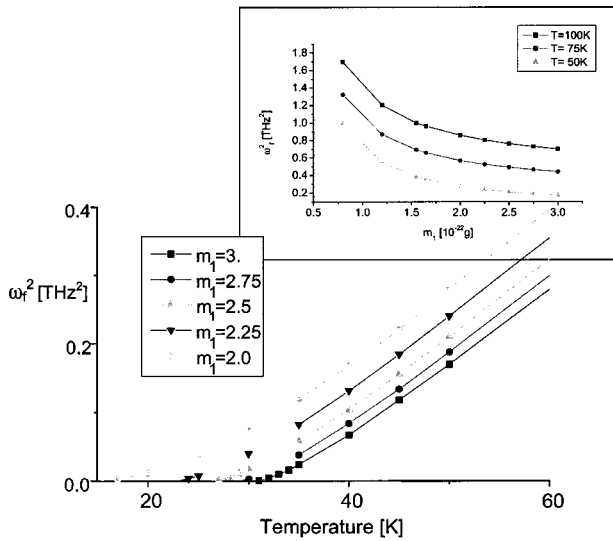


FIG. 2. Temperature dependence of the square of the soft mode frequency for varying mass  $m_1$ . The inset shows the squared soft mode frequency as function of  $m_1$  at different temperatures.

while the Curie constant becomes strongly mass dependent. A comparison to perovskite ferroelectrics is possible here only if  $g_2$  and  $g_4$  do not change with changing mass  $m_2$ . This is, however, mostly not the case, since the experimentally determined temperature dependencies of the soft modes vary considerably from compound to compound, and it is just this temperature behaviour which yields the self-consistent values of  $g_2$  and  $g_4$ . Correspondingly our results are not applicable to replacing, e.g., Sr in  $\text{SrTiO}_3$  by Ba. Instead these results apply to systems where the A ion sublattice mass is replaced by its isotope, and it is hoped that corresponding experiments will be performed in the future.

A mass-dependent phase diagram can be constructed by calculating, for given mass, the critical value of  $g_2$  at which the ferroelectric instability takes place (Fig. 4). While, as expected from Fig. 3, the variation of  $m_2$  has nearly no effect on the phase diagram, changes in  $m_1$  are crucial to the existence regime of both phases. For small  $m_1$  quantum fluctuations dominate the dynamics. In addition the critical value  $|g_2|$  increases strongly in this limit indicative of a crossover

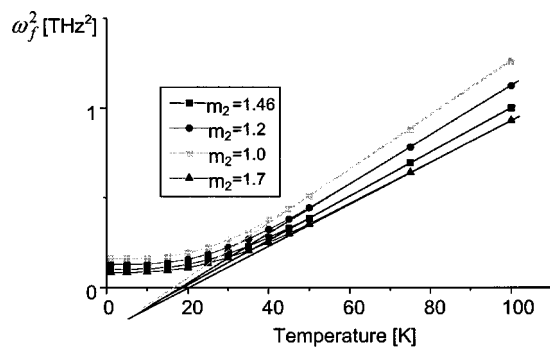


FIG. 3. Temperature dependence of the squared soft mode frequency for varying mass  $m_2$ . The straight lines correspond to extrapolations from the high-temperature regime and their intersections with the temperature axis define  $T_{c,\text{extrapolated}}$ .

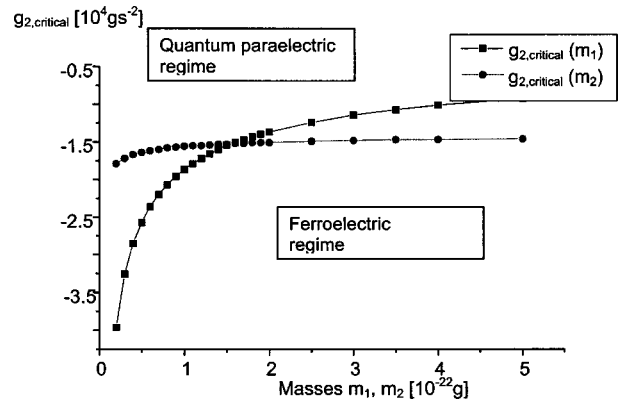


FIG. 4. The phase diagram of the quantum fluctuation dominated regime and the ferroelectric regime as a function of the involved masses  $m_1, m_2$ . The value  $g_{2,\text{critical}}$  defines the potential barrier height at which a ferroelectric state appears.

from displacive to order-disorder dynamics. In this regime ferroelectricity can easily be induced by small variations in  $m_1$ .

On the other hand, in the displacive limit the mass dependence is less pronounced and nearly vanishes for sufficiently large  $m_1$ . Obviously small masses more easily facilitate tunneling dynamics between the potential wells and freezing into either of the wells at the critical temperature than heavy units which follow the displacive soft mode dynamics with a much longer time scale. The crucial role of the polarizable sublattice mass for the phase diagram can be further investigated by comparing the onset temperature of quantum fluctuations, i.e., the deviations from the high-temperature behavior of the soft mode, with the extrapolated meanfield  $T_{c,\text{extrapolated}}$ , respectively, the real instability point  $T_c$ , where  $|g_2|$  is larger than the critical value beyond which a ferroelectric instability sets in. This is shown in Fig. 5. A new regime in the phase diagram appears which is dominated by quantum fluctuations but simultaneously carries polar character due to the proximity to the ferroelectric state. We term this a “polar quantum” state. In this state the elastic properties are

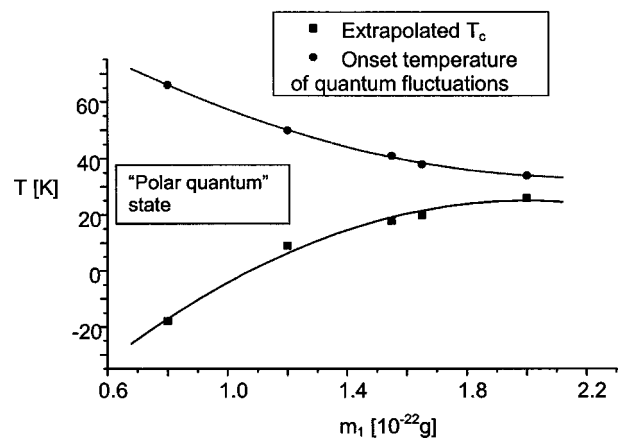


FIG. 5. The high-temperature extrapolated  $T_{c,\text{extrapolated}}$  and the temperature at which quantum fluctuations set in, i.e., the temperature where deviations from meanfield behavior occur, as functions of  $m_1$ .

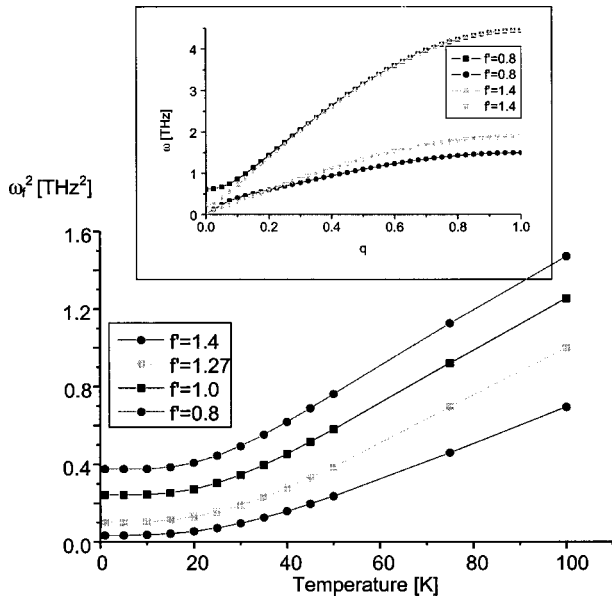


FIG. 6. Temperature dependence of the squared soft mode frequency for various values of  $f'$ . The inset shows the lowest two lattice modes as a function of wave vector  $q$  for the largest and smallest value of  $f'$  in the figure.

anomalous<sup>19</sup> and indicative of the formation of preformed polar clusters. With increasing mass  $m_1$ , which corresponds to a stabilization of the polar instability, the new phase decreases and the phase boundary lines merge.

As can be seen in Fig. 5, quantum fluctuations are not restricted to small temperatures but can be present at rather high temperatures if the polarizable mass is small. In this regime an unexpected and interesting role is played by the core-core coupling between the polarizable units  $f'$ , which determines the elastic properties of the material since in the limit  $q \rightarrow 0$  the acoustic mode is given by  $\omega_{TA}^2(q \rightarrow 0) \cong 4f'q^2a^2/m_1$ . As is obvious from Eq. (4), the soft mode itself does not depend directly on  $f'$  but only indirectly from the dynamical information provided through Eq. (2). On the other hand, pronounced optic acoustic mode coupling is known to set in in the vicinity of the phase transition, since there the optic mode approaches the acoustic mode limit. Stiffening the interaction between the polarizable units then

has competing effects on the dynamics since it would lead to complete electron localization at finite wave vector, i.e., charge-density-wave formation, but this is inhibited by the soft mode induced precursor effects. Increases in  $f'$ , “stiffening,” lead to dramatic decreases in  $g_T$ , which brings the system to its stability limit where optic and acoustic modes start mixing (Fig. 6). This in turn induces anomalies in the acoustic mode dispersion at small wave vectors which crucially affect the elastic properties (see inset to Fig. 6). Thus the stiffening has the paradoxical role of simultaneously softening not only the transverse optic mode but also inducing elastic softening on new length scales. Experimentally, exactly this behavior has been observed—not in the quantum limit but in the vicinity of the structural phase transition—in  $\text{PbTiO}_3$  (Ref. 20) where an increased softening of the soft mode occurs close to  $T_c$  coinciding with anomalies in the transverse acoustic branch at small wave vector. Varying the core-shell coupling  $f$  has no effect at all on the soft mode or the Curie constant, since the selfconsistency loop [Eqs. (4) and (2)] automatically adjusts the value of  $g_T$  to keep  $\omega_f^2$  constant.

In conclusion, we have studied the existence regimes of quantum fluctuations in ferroelectric systems as functions of the double-well potential barrier height, the masses, and the elastic properties. While the variation of the rigid sublattice mass has nearly no effect on the phase diagram, the role played by the polarizable mass is crucial: it defines not only the phase boundary between the polar and the quantum paraelectric state, but also governs the dynamics, which are driven from displacive to order-disorder with decreasing mass  $m_1$ . A phase is observed when  $m_1$  is varied wherein quantum fluctuations *coexist* with polar precursor dynamics evidenced by anomalies in the elastic constants.<sup>19</sup> An interesting role is found to be played by the elastic properties of the system: a stiffening interaction between the cluster masses induces strong softening of the optic mode in addition to anomalies of elastic constants on new length scales. The stiffening also induces a strong competition between charge-density-wave formation and ferroelectricity, but the latter always prevails. A stabilization of the dielectric constant at rather high values and over a broad temperature interval can be obtained in this regime and also in the limit of small masses  $m_1$ .

<sup>1</sup>See, e.g., J. F. Scott and C. A. Araujo, *Science* **246**, 1400 (1989).

<sup>2</sup>C. C. Homes, T. Vogt, S. M. Shapiro, S. Wakimoto, and A. P. Ramirez, *Science* **293**, 673 (2001).

<sup>3</sup>K. A. Müller and H. Burkard, *Phys. Rev. B* **19**, 3593 (1979).

<sup>4</sup>U. T. Höchli, H. E. Weibel, and L. A. Boatner, *Phys. Rev. Lett.* **39**, 1158 (1977).

<sup>5</sup>R. Morf, T. Schneider, and E. Stoll, *Phys. Rev. B* **16**, 462 (1977).

<sup>6</sup>M. Itoh, R. Wang, Y. Inaguma, T. Yamaguchi, Y.-J. Shan, and T. Nakamura, *Phys. Rev. Lett.* **82**, 3540 (1999).

<sup>7</sup>A. Bussmann-Holder, H. Büttner, and A. R. Bishop, *J. Phys.: Condens. Matter* **12**, L115 (2000).

<sup>8</sup>J. H. Barrett, *Phys. Rev.* **86**, 118 (1952).

<sup>9</sup>T. Schneider, H. Beck, and E. Stoll, *Phys. Rev. B* **13**, 1123 (1976).

<sup>10</sup>H. Bilz, G. Benedek, and A. Bussmann-Holder, *Phys. Rev. B* **35**, 4840 (1987).

<sup>11</sup>R. E. Cohen and H. Krakauer, *Phys. Rev. B* **42**, 6416 (1990).

<sup>12</sup>W. Zhong, David Vanderbilt, and K. M. Rabe, *Phys. Rev. B* **52**, 6301 (1995).

<sup>13</sup>C. Perry *et al.*, *Phys. Rev. B* **35**, 8666 (1989); R. L. Migoni, K. H. Rieder, K. Fisher, and H. Bilz, *Ferroelectrics* **13**, 377 (1976); G. Khatib, R. L. Migoni, G. E. Kugel, and L. Godefroy, *J. Phys.:*

- Condens. Matter **1**, 9811 (1991); G. E. Kugel, M. D. Fontana, and W. Kress, Phys. Rev. B **35**, 813 (1987); M. Stachiotti and R. L. Migoni, J. Phys.: Condens. Matter **2**, 4341 (1990); M. Stachiotti, R. L. Migoni, and U. T. Höchli, *ibid.* **3**, 3689 (1991); A. Bussmann-Holder, H. Bilz, and G. Benedek, Phys. Rev. B **39**, 9214 (1989).
- <sup>14</sup>K. H. Weyrich, Ferroelectrics **79**, 65 (1988).
- <sup>15</sup>R. Migoni, H. Bilz, and D. Bäuerle, Phys. Rev. Lett. **37**, 1155 (1976).
- <sup>16</sup>G. Benedek, A. Bussmann-Holder, and H. Bilz, Phys. Rev. B **36**, 630 (1987).
- <sup>17</sup>H. Bilz, H. Büttner, A. Bussmann-Holder, W. Kress, and U. Schröder, Phys. Rev. Lett. **48**, 264 (1982).
- <sup>18</sup>A. Bussmann-Holder and A. R. Bishop, Phys. Rev. B **56**, 5297 (1997).
- <sup>19</sup>A. Bussmann-Holder, H. Büttner, and A. R. Bishop, in *Fundamental Physics of Ferroelectrics 2002*, edited by Ronald E. Cohen, AIP Conf. Proc. No. 626 (AIP, Melville, 2002), p. 141.
- <sup>20</sup>G. Shirane, J. D. Axe, J. Harada, and J. P. Remeika, Phys. Rev. B **2**, 155 (1970).